Supporting information

Linear, redox modified DNA probes as electrochemical DNA sensors†

Francesco Ricci [a c], Rebecca Y. Lai [a b] and Kevin W. Plaxco [a *]

Receipt/Acceptance Data **[DO NOT ALTER/DELETE THIS TEXT]**
Publication data **[DO NOT ALTER/DELETE THIS TEXT]**
DOI: 10.1039/b000000x [DO NOT ALTER/DELETE THIS TEXT]

MATERIALS AND METHODS

Probe DNA and Sensor Fabrication.

Reagent grade chemicals, including 6-mercapto-1-hexanol (C_6-OH), iron-supplemented fetal calf-serum, sulfuric acid (all from Sigma-Aldrich, St. Louis, MO), potassium phosphate monobasic, dibasic, and sodium chloride (Fisher Scientific) were used without further purification. A 27-base, 3' thiol-, 5' methylene blue (MB)-modified oligonucleotide was obtained from Biosearch Technologies (Novato, CA) and employed as the probe DNA. The 17 internal bases of this sequence are complementary to the *gyrB* gene of *Salmonella*. Flanking the *gyrB* sequence are two copies of a 5-base element identical to the 3' end of the stem-loop structure we have employed in previous E-DNA studies. [1 2] The MB redox moiety was conjugated to the 3' end of the oligonucleotide via succinimide ester coupling to a 3' amino modification (MB-NHS, EMP Biotech, Berlin) producing the probe sequence: 5'-HS-$(CH_2)_6$-CGTCAATCTTCTATTTCTCCACACTGC-$(CH_2)_7$-NH-MB-3'.

The sensors were fabricated on rod gold disk electrodes (2.0 mm diameter, BAS, West Lafayette, IN). The electrodes were prepared by polishing with diamond and alumina (BAS), followed by sonication in water, and electrochemical cleaning (a series of oxidation and reduction cycles in 0.5 M H_2SO_4, 0.01 M KCl/0.1 M H_2SO_4, and 0.05 M H_2SO_4). The effective area of the electrode was determined from the charge associated with the gold oxide reduction peak obtained after the cleaning process and a roughness factor (the ratio of the real to apparent or geometric electrode area) of ~1.11 was typically observed. The probe DNA was immobilized onto these freshly cleaned electrodes by incubating for one hour in a solution of 1 μM TCEP (Tris(2-carboxyethyl) phosphine hydrochloride) in 100 mM NaCl/10 mM potassium phosphate pH 7 buffer containing the appropriate concentrations of probe DNA. Different probe densities were obtained by controlling the concentration of probe DNA employed during the fabrication process. Following probe immobilization the electrode surface was rinsed with distilled, di-ionized water and subsequently passivated with 1 mM 6-mercaptohexanol in 1 M NaCl/10 mM potassium phosphate buffer, pH 7, for 2 hr. and followed by further rinsing with deionized water.

Target DNA Sequences.

We employed target DNA sequences of varying lengths and structures (Table S1), all of which were obtained via commercial synthesis (Sigma Genosys, St. Luis, MO). The target sequences were as follows:

ST-25 (normal target, 17 bases, 5'- GTG GAG AAA TAG AAG AT – 3'); ST-25-3M1 (three T-T mismatched target, 17 bases, 5'- GTG GAG TTT TAG AAG AT – 3'); LT-27 (27 bases target, 5'- GCAGT GTG GAG AAA TAG AAG AT TGACG– 3'); MLL-38 (long target with a structured loop tail, 38 bases, 5'- GCGTTTTTCGC GCAGT GTG GAG AAA TAG AAG AT TGACG – 3').

Electrochemical Measurements.

The sensor response was measured by incubating the electrodes in 200 nM of the appropriate target DNA. The sensors were interrogated at different intervals in the same target solution until a stable current peak was obtained. The ratio between the stabilized current peak in the presence of target DNA and the current peak in absence of target DNA gives the measure of the signal suppression caused by the target. Before being used to detect the next target the electrodes were rinsed with deionized water and interrogated in target free buffer. This also provides a measure of the extent to which each sensor can be regenerated. When fetal calf serum was used it was diluted 1:1 with buffer solution. Prior to interrogation, the electrodes were incubated for ~30 min. in the sample lacking exogenously added target. The target was added only when the sensor had fully equilibrated/stabilized as determined by stable peak currents. The sensor was then allowed to incubate in the presence of the target for ~30 min. before voltammetric measurements were conducted directly in the sample. Sensor regeneration was achieved via immersing in 10% SDS for 2 min followed by rinsing with deionized water. Regeneration was verified by ACV collected after 30 min. immersion in target-free buffer/serum solution.

All measurements were performed at room temperature using a CHI 730B Electrochemical Workstation (CH Instruments, Austin, TX). Alternating current voltammograms (ACV) were recorded from –0.05 V to –0.44 V *vs*. an Ag/AgCl (3 M NaCl) reference

[a] *Department of Chemistry and Biochemistry, University of California, Santa Barbara, California 93106.*
[b] *Department of Physics and Institute for Polymers and Organic Solids, University of California, Santa Barbara, California 93106.*
[c] *On leave from the University of Rome Tor Vergata, Dipartimento di Scienze e Tecnologie Chimiche, Via della Ricerca Scientifica, 00133, Rome, Italy.*

† *Electronic Supplementary Information (ESI) available: [Experimental procedures, controlling probe surface density, sensor equilibration time and specificity, the effect of target length and bulk on signaling, electron transfer rate measurements, and probe density effects on signaling].*

electrode in a standard cell with a platinum counter electrode. All experiments were conducted using a 25 mV AC potential at a frequency of 10 Hz unless otherwise stated. All experiments were conducted in 1 M NaCl/10 mM potassium phosphate buffer, pH 7. Probe surface density (*i.e.,* the number of electroactive probe DNA moles per unit area of the electrode surface, N_{tot}) was determined using a previously established relationship with ACV peak current[3] described in equation (1):

Eq 1
$$I_{avg}(E_0) = 2nfFN_{tot}\frac{\sinh(nFE_{ac}/RT)}{\cosh(nFE_{ac}/RT)+1}$$

where: $I_{avg}(E_0)$ is the average ac peak current in voltammogram, n is the number of electrons transferred per redox event (with our MB label n = 2), F is the Faraday current, R is the universal gas constant, T is the temperature, E_{ac} is the peak amplitude, and f is the frequency of the applied AC voltage perturbation. Perfect transfer efficiency was assumed (*i.e.,* that all of the redox moieties participate in electron transfer); errors in this assumption would lead us to underestimate probe density. Experimentally, 4 different frequencies were used (5, 10, 50, and 100 Hz) and the average current peak was calculated so as to give the value of N_{tot}.

Electron Transfer Rate Measurements.

The study of electron transfer rate was performed using ACV at frequencies ranging from 0.1 to 10,000 Hz. The peak current was then evaluated for each frequency and the ratio between the current peak and the baseline current was plotted vs. the measurement frequency.[4 5] The study was performed before and after the hybridization with 200 nM target DNA.

Notes and references

1 C. Fan, K.W. Plaxco and A.J. Heeger, *Proc. Natl. Acad. Sci. USA*, 2003, **100**, 9134.

2 R.Y. Lai, E.T. Lagally, S.-H. Lee, H.T. Soh, K.W. Plaxco and A.J. Heeger, *Proc. Natl. Acad. Sci. USA*, 2006, **103**, 4017.

3 S.D. O'Connor, G.T. Olsen and S.E. Creager, *J. Electroanal. Chem.* 1999, **466**, 197.

4 S.E. Creager and T.T. Wooster, *Anal. Chem.* 1998, **70**, 4257.

5 J.J. Sumner, K.S. Weber, L.A. Hockett and S.E. Creager, J. Phys. Chem. B 2000, 104, 7449.

6 P. Gong, C.-Y. Lee, L.J. Gamble, D.G. Castner and D.W. Grainger, *Anal. Chem.* 2006, **78**(10), 3326.

7 A.W. Peterson, R.J. Heaton and R.M. Georgiadis, *Nucleic Acids Res.* 2001, **29**, 5163.

8 A.W. Peterson, L.K. Wolf, R.M. Georgiadis, *J. Am. Chem. Soc.* 2002, **124**, 14601.

9 F. Ricci, R.Y. Lai, A.J. Heeger, K.W. Plaxco, K. W. and J.J. Sumner, *Langmuir*, 2007, **23**(12), 6827.

Table SI1 Summary of E-DNA sensor performance.

Sensor	Probe DNA concentration used during sensor fabrication (μM)	Probe density (molecules/cm^2)	Mean probe-to-probe separation (nm)	ACV i_p (nA)	Signal suppression with ST-25 (%)	Selectivity ratio [a]	Average regeneration[b] (%)
HIGH DENSITY	0.5	1.6×10^{12}	8.0	440	85 ± 2	1.17	97 ± 2
MEDIUM DENSITY	0.1	4.2×10^{11}	15.4	110	60 ± 2	1.05	98 ± 3
LOW DENSITY	0.02	5.1×10^{10}	44.5	10	58 ± 3	1.00	94 ± 3

[a] Ratio between the signal suppression obtained with the complementary target (ST-25) and a three-bases mismatched target (ST-25-3M1).

[b] Signal recovery after target hybridization obtained rinsing with deionised water and testing in target free buffer. Values are the average and standard deviation of measurements performed with three independent sensors.

Table SI2 Effects of Target Length and Bulk on Signal Suppression

DNA TARGET	ST-25	LT-27	MLL-38
BINDING SCHEME [a]	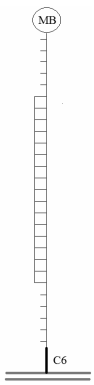	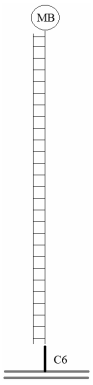	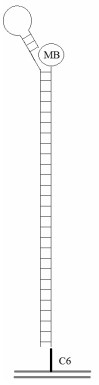
HIGH DENSITY [b] 1.6×10^{12} molecules/cm^2	85 ± 2	94 ± 1	91 ± 2
MEDIUM DENSITY 4.2×10^{11} molecules/cm^2	60 ± 2	88 ± 3	97 ± 3
LOW DENSITY 5.1×10^{10} molecules/cm^2	58 ± 3	88 ± 3	100 ± 1

[a] See table S1 for sequences.
[b] % values of signal suppression as a result of target hybridization are the average and standard deviation of measurements performed with four independent sensors.

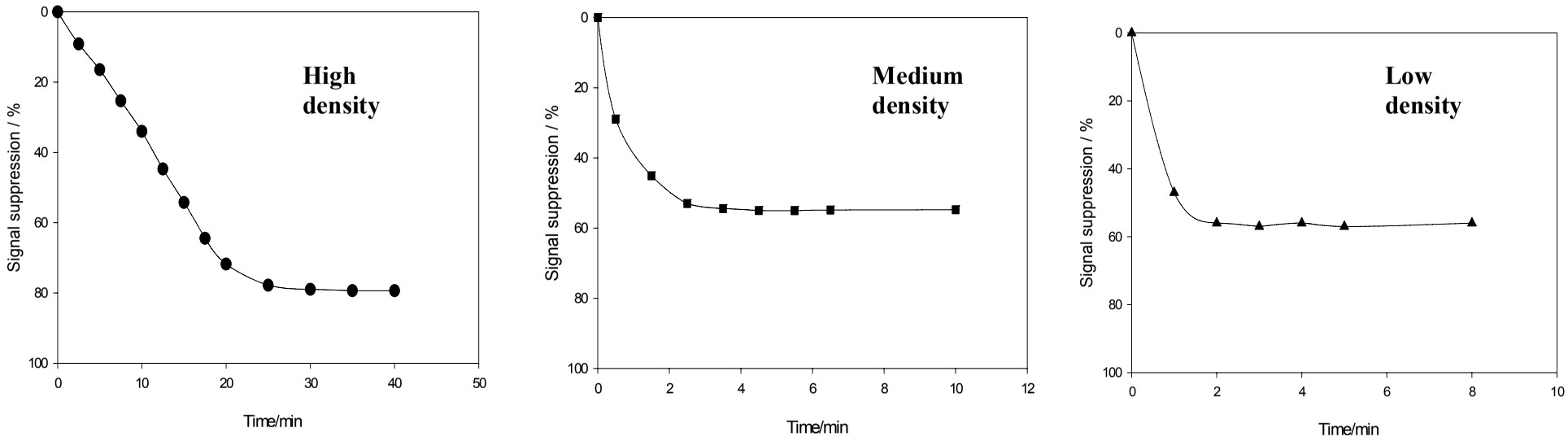

Figure SI1. Sensor equilibration time is dependant on probe density. Shown is the response to the presence of 200 nM target DNA (ST-25) of three representative sensors with high (1.6 x 10^{12} molecules/cm^2) medium (4.2 x 10^{11} molecules/cm^2) and low (5.1 x 10^{10} molecules/cm^2) density.

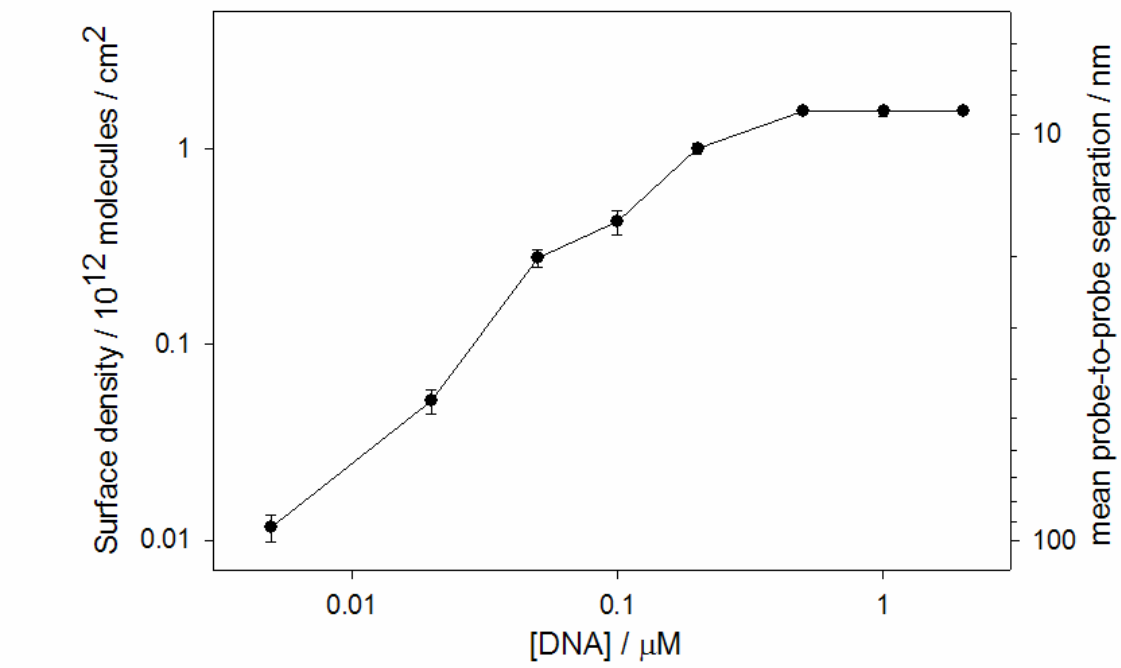

Figure SI2. Probe density affects the E-DNA signaling and equilibration time and provides insights into the details of the sensing mechanism. We have controlled probe density by changing the concentration of probe DNA employed during sensor fabrication. Using this approach we can readily and reproducibly fabricate linear-probe sensors with probe densities ranging from 1.2 x 10^{10} to 1.6 x 10^{12} molecules/cm^2 (corresponding to packing of 2.0 x 10^{-14} to 2.6 x 10^{-12} mol/cm^2) by employing probe DNA concentrations from 0.005 to 2 μM during fabrication. Attempts to fabricate sensors with lower probe densities fail to produce stable, active films and no electrochemical signal is detectable (data not shown). The observed probe density increases monotonically with increasing probe concentration until a density of ~1.6 x 10^{12} molecules/cm^2 is obtained, after which no further increases in probe density are observed. Similar saturating probe densities have been reported by others using comparable length linear probes[6-8] and by similar approach using an equivalent stem-loop probe.[9]Values and error bars respectively represent the average and standard deviation of measurements conducted with three independently fabricated sensors.

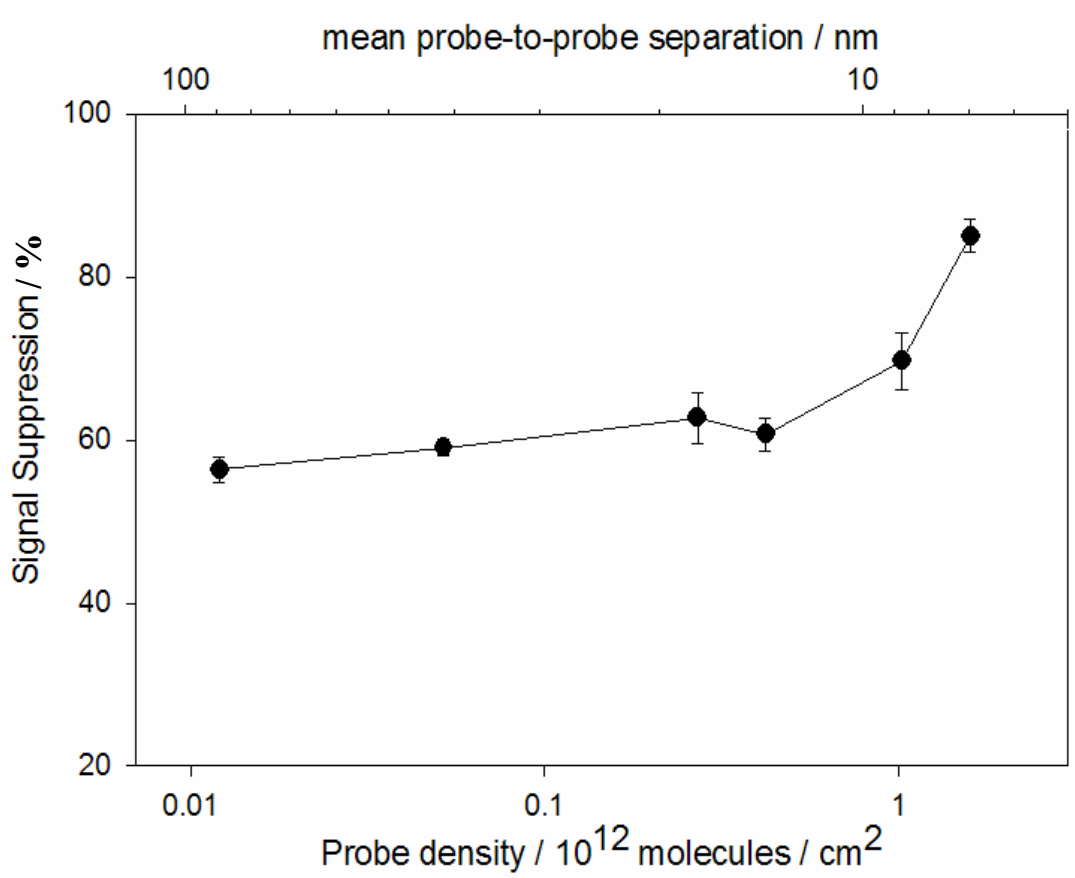

Figure SI3. Probe-density-dependence of linear probe E-DNA signaling is complex. At the saturating probe density of 1.6 x 10^{12} molecules/cm^2 we observe 85 % suppression. Reduction of the probe density to 4.2 x 10^{11} molecules/cm^2 reduces the signal suppression to 60%, a level that is maintained as the probe density drops to the lowest values we can readily measure. The transition between these two regimes is quite sharp: a change in the probe density of ~3 fold (from 1.6 x 10^{12} to 4.2 x 10^{11} molecules/cm^2) gives rise to a 1.5-fold increase in signal suppression. Shown is the dependence observed at 200 nM target DNA (ST-25). Values represent the average and standard deviation of measurements conducted with three independent sensors at each surface density.

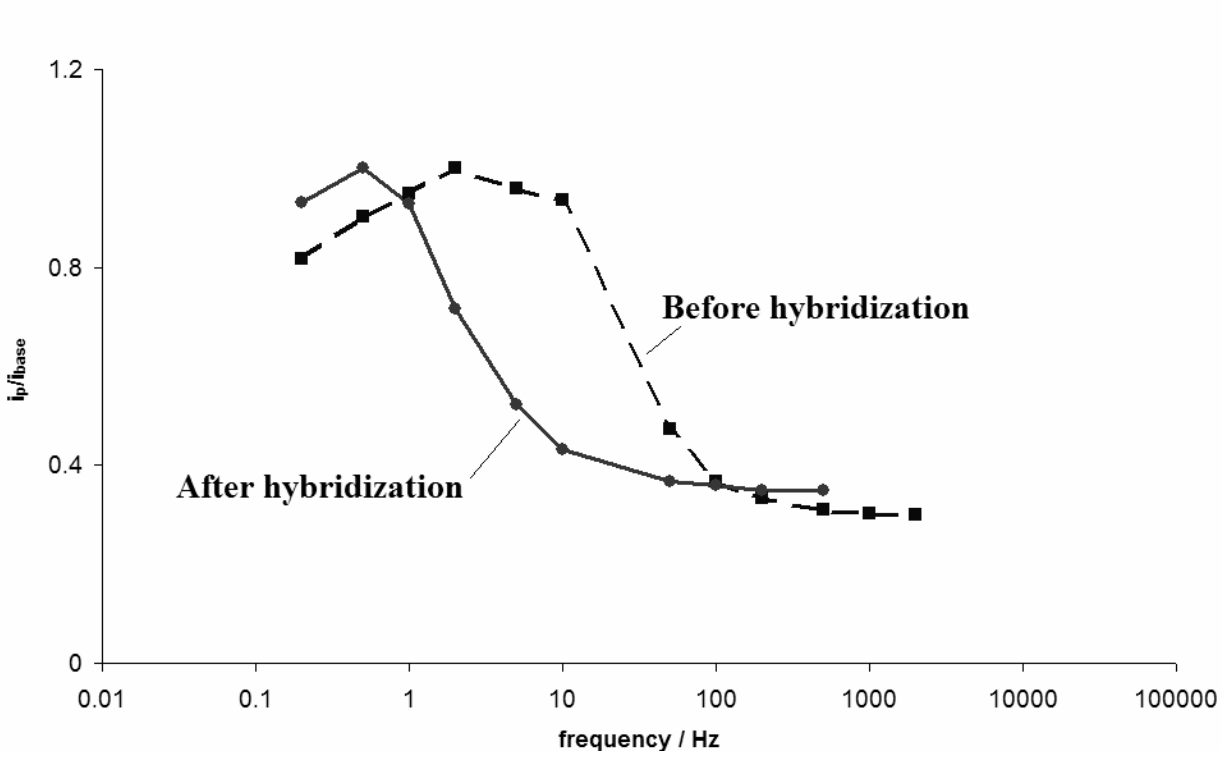

Figure SI4. Observed electron transfer rates differ for hybridized and un-hybridized probes. A sharp change in the slope of the i_p/i_{base} values is observed as the AC frequency is increased and the electron transfer rate is no longer rapid enough to keep pace with the oscillating applied potential, reflecting the collision-limited transfer rate of the hybridized probe-target duplex.

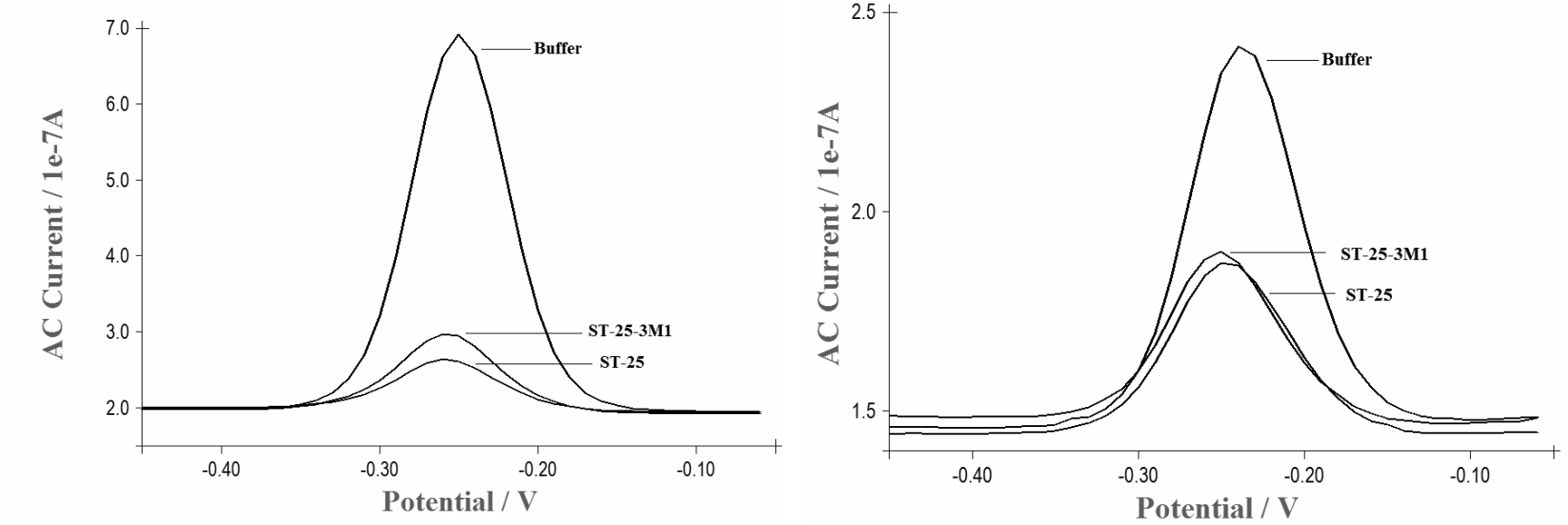

Figure SI5. Specificity of the sensor is somewhat sensitive to probe density. Representative ACVs obtained with high (1.6×10^{12} molecules/cm^2 - left) and medium (4.2×10^{11} molecules/cm^2 - right) density sensors indicate that higher density sensors are better able to discriminate a three-bases mismatched target (ST-25-3M1).

Table SI3: Probe and target sequences

DNA	Sequence[a]	Number of bases	Description
PROBE	5'-C6-S-S-CGTCAATCTTCTATTTCTCCACACTGC-MB-3'	27	Probe modified with MB
ST-25	5'-GTG GAG AAA TAG AAG AT–3'	17	Complementary target with 17 bases
ST-25-3M1	5'-GTG GAG TTT TAG AAG AT–3'	17	Three contiguous mismatches
LT-27	5'-GCAGT GTG GAG AAA TAG AAG AT TGACG–3'	27	Complementary target with 27 bases
MLL-38	5'-*GCGTTTTTCGC* GCAGT GTG GAG AAA TAG AAG AT TGACG–3'	38	Target complementary with 17 bases and a 11 bases tail forming a loop

[a] Underlined bases are those different from the normal target so they indicate mismatches and elongation of the target. Bases in *italic* are designed to form a structured loop.

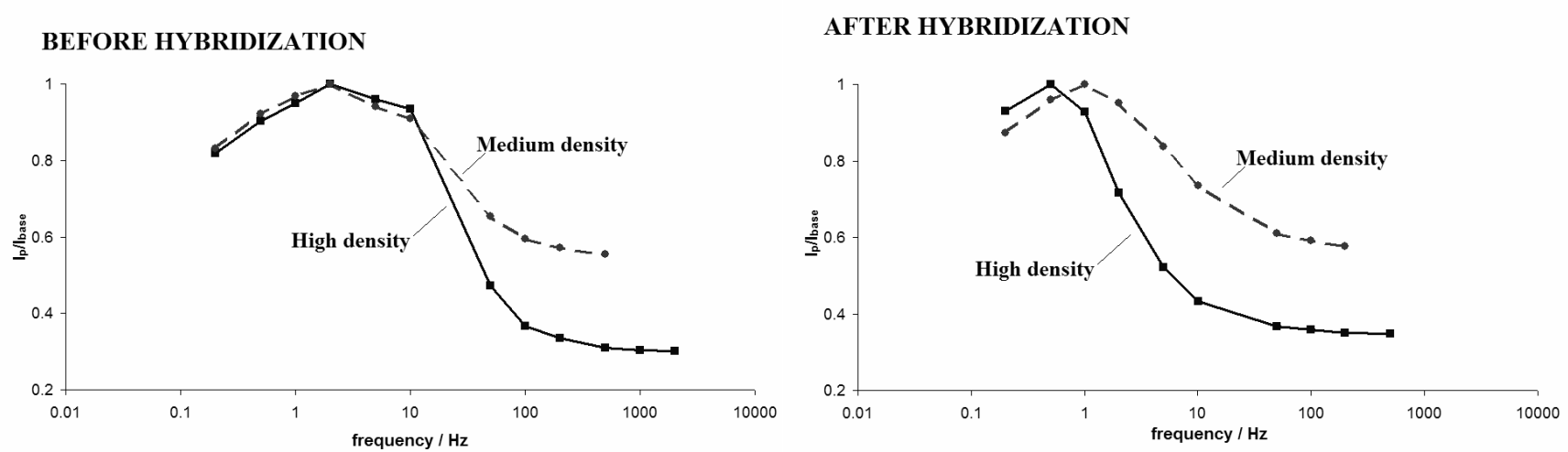

Figure SI6. The dependance of i_p/i_{base} on ACV frequency differs for higher and lower-density sensors. Before hybridization, both high and medium density sensors respond similarly to frequency changes and a comparable electron transfer rate is observed (left). Upon hybridization, the electron transfer rate of higher density sensors is reduced significantly relative to those of medium density sensors, probably accounting for the higher signal suppression observed for the latter (right). This presumably reflects the effects of crowding on the collision rate between the electrochemical label and the electrode surface.